

Dynamic Behavior of Rack Vehicle System Subject to Gravity Center Offset

Mi'ao YUAN*, Zhaowei CHEN**, Shihui LI***, Zhihui CHEN****, Jizhong YANG*****

*Chongqing Vocational College of Transportation, Chongqing, China; No. 555 Xiangfu Avenue, Shuangfu Street, Jiangjin Dist, Chongqing, China, E-mail: yma14789@foxmail.com (Corresponding Author)

**School of Mechatronics & Vehicle Engineering, Chongqing Jiaotong University, Chongqing, China; School of Mechatronics & Vehicle Engineering, Chongqing Jiaotong University, No.66 Xuefu Rd, China, E-mail: chenzhaowei_cq@163.com

***School of Mechatronics & Vehicle Engineering, Chongqing Jiaotong University, Chongqing, China; School of Mechatronics & Vehicle Engineering, Chongqing Jiaotong University, No.66 Xuefu Rd, China, E-mail: lishihui_cq@163.com

****Science and Technology Research Institute, China Railway Eryuan Engineering Group Co.Ltd, Chengdu, China; School of Mechatronics & Vehicle Engineering, Chongqing Jiaotong University, No.66 Xuefu Rd, China, E-mail: 1683990279@qq.com

*****Science and Technology Research Institute, China Railway Eryuan Engineering Group Co.Ltd, Chengdu, China; School of Mechatronics & Vehicle Engineering, Chongqing Jiaotong University, No.66 Xuefu Rd, China, E-mail: 2281638726@qq.com

<https://doi.org/10.5755/j02.mech.39989>

1. Introduction

The Washington Mountain Railway in the United States is the world's first rack railway which completed its first passenger transport in 1868 [1], and now rack railways are widely used in Europe. In China, Dujiangyan, Jiuzhai-gou and Zhangjiajie are also preparing to build rack railway with Strub system as the main system. In 2019, Sichuan Province promulgated the Technical Code of Mountain (Rack) Rail Transit, which further promoted the development of rack railway in China. Rack vehicle are mostly used in complex and steep terrain areas [2], and gravity center of the carbody is easily offset due to line inclination and environmental disturbance in such a bad transportation process. The offset of the carbody gravity center not only causes the rotational inertia of the vehicle body and the balance position of the system to change, but also induces uneven suspension force and lateral displacement of the wheelset. These phenomena seriously affect the dynamic meshing of gear-rack and disturbs the wheel/rail nonlinear contact behavior [3], eventually leading to serious accidents such as equipment damage or vehicle derailment and subversion during the transportation of rack vehicles. Therefore, it is necessary to carry out in-depth research on the influence of the offset of gravity center on the dynamic characteristics of the rack vehicle system.

At present, scholars have conducted very few investigations on the dynamic characteristics of rack vehicle with gravity center offset. This paper mainly reviews the relevant research on the running characteristics of rack vehicle and the gear-rack nonlinear dynamics, and summarizes the basic theory and technology of rack vehicle. In order to improve the safety and stability of rack vehicles during transportation, some scholars have explored the impact of different transportation conditions on rack vehicle from the perspective of multi-body dynamics. Liu et al. [4] studied the influence of different gear parameters on the impact vibration of rack vehicle. Chen et al. [5] considered the gear rack nonlinear meshing and studied the influence of different

traction motor layout modes on the rack vehicle system. Guo et al. [6] studied the influence of gear meshing on the fatigue life of high-speed railway vehicle bogie frame based on rigid flexible coupling dynamics. Chen et al. [7] propose a method to analysis the nonlinearity and non-stationarity of dynamic response of high-speed vehicle-track coupling system, to understand the properties of signal and its underlying physical meaning. Ha et al. [8] studied the influence of softening cement asphalt mortar on the operation safety and dynamic characteristics of high-speed railway. Wang et al. [9] studied the effect of the nonlinear displacement-dependent characteristics of a hydraulic damper on high-speed rail pantograph dynamics. Zhang et al. studied the dynamic response of vehicles on dip-joint and corrugation rails [10]. From the above research, we can know that different structural forms and line conditions have a great impact on the operation safety and stability of rail vehicles. The rack vehicle is driven by the gear-rack meshing, and the gear-rack meshing introduce new excitation for the operation of the rack vehicle. Yu et al. [11] explored the influence of spatial crack propagation of spur gear teeth on gear meshing stiffness. Wei et al. [12] studied the dynamic response of a single-mesh gear system with periodic mesh stiffness and backlash nonlinearity under uncertainty. Cooley et al. [13] compared several gear meshing stiffness calculation methods and analyzed the unique uses of each calculation method. Pei et al. [14] studied the lubrication reliability of a gear pair excited by different intensity random load. Chen et al. [15] studied the reliability of shearer permanent magnet semi-direct drive gear transmission system in combination with the nonlinear fatigue damage theory. He et al. [16] through the contact collision algorithm of multi-body dynamics, analyze the change regularity of meshing force and output speed of the different pit morphology face gear transmission under certain condition. Neusser et al. [17] predicted and analyzed the gear dynamics and transmission error of the gear meshing model based on multi-body dynamics. The gear meshing is obviously affected by the working conditions can be found from the above research. However,

the rack vehicle operation environment is complex, so it is necessary to study the dynamic characteristics of rack vehicles driven by gear nonlinear meshing. In addition, some scholars have studied the operation characteristics of rail vehicles under the offset of the carbody gravity center. Bao et al. [18] studied the relationship between the derailment coefficient of C70 gondola and the lateral offset of the center of gravity. Wan et al. [19] studied the influence of carbody gravity center deviation on transverse vibration of freight cars on curved track. Zhang et al. [20] studied the effect of mass distribution on curving performance for a loaded wagon. Li et al. [21] took D5 truck as an example to analyze the relationship between vehicle loading utilization and allowable lateral offset. As concluded from the above studies that the gravity center offset of carbody has a significant impact on the dynamic characteristics of traditional rail vehicle operation, but there are little literatures on the impact on rack vehicle system.

This research aims at the influence of the carbody gravity center offset on the dynamic characteristics of rack vehicles, and the mechanism of the gear-rack dynamics nonlinear meshing disturbance is analyzed. On this basis, the coupling dynamics model of the rack vehicle system is established according to the Strub rack system, which with the consideration of offset of the carbody gravity center. Using this model, considering the gear-rack time-varying meshing disturbance in combination with the structural characteristics of the rack vehicle. The effect of the carbody gravity center offset on the gear-rack nonlinear meshing behavior and wheel/rail dynamic contact force when the rack vehicles operate on a slope at different speeds is researched. Based on this research, the safety and stability of rack vehicle at different speeds under the offset of the carbody gravity center are analyzed.

2. Dynamic Model of Rack Vehicle Subject to Carbody Gravity Center Offset

The structure of the rack vehicle is briefly explained in this chapter, and on this basis, the rack vehicle is expressed in mathematics and mechanics to form a dynamic model of the rack vehicle system.

The research method is shown in the Fig. 1. Firstly, according to Gear dynamics and Multi-body theory, the gear-rack meshing model and rack-vehicle coupling model are established. Secondly, the gear-rack meshing effect is analyzed, and the wheel/rail nonlinear friction contact behavior is explored under the condition of center of gravity offset. Finally, the effect of gear-rack meshing on vehicle safety and stability is analyzed.

2.1. Rack vehicle structure

Rack vehicles are similar to traditional rail vehicles. They are composed of carbody, driving system, running system, braking system, connecting system. However, the driving method is different from that of traditional rail vehicle. As shown in Fig. 2, the Strub rack system lays a rack between the two rails, and installs the driving gear on the axle to supplement or replace the insufficient wheel rail adhesion when the vehicle running at slope section.

2.2. Coupling dynamic model of rack vehicle system

The construction of the rack vehicle system coupling model is the basis for studying the influence of the gravity center offset on the rack vehicle system. This section introduces the establishment of the rack vehicle dynamics model, gear-rack meshing model and the rack vehicle carbody gravity center offset model in detail.

According to the structure of the rack vehicle, the key structures and components such as wheelset, rail, driving gear and rack are considered in detail. The established rack vehicle dynamic model is shown in Fig. 3. It should be noted that this subsection focuses on the rack vehicle dynamic model, while the gear-rack meshing model is described in detail in the next subsection.

All parts of rack vehicle can be considered as a multi rigid body system [22]. The degree of freedom (DoF) of the rack vehicle in the model is 47, as shown in Table 1. According to vehicle coupling dynamics and gear dynamics, and the differential equation of motion of the system can be obtained by the D'Alembert principle to each rigid body one by one. The motion equation matrix of rack vehicle can be deduced as follows.

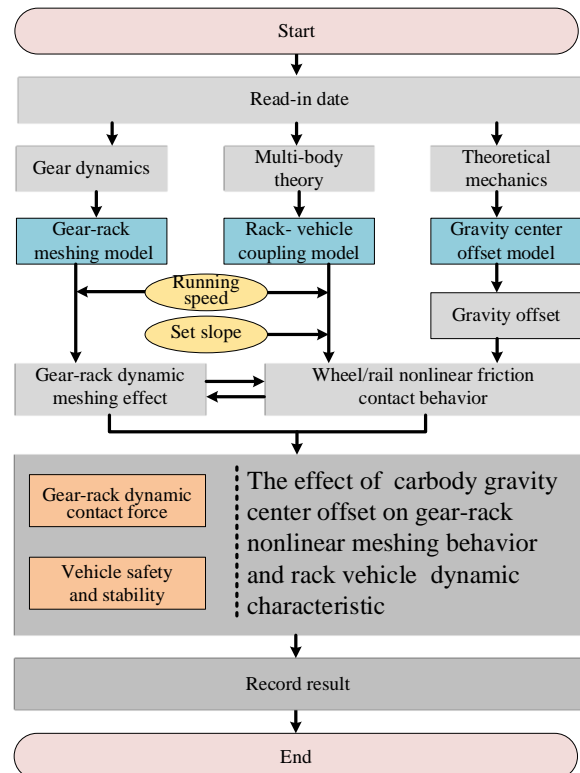


Fig. 1 Research method

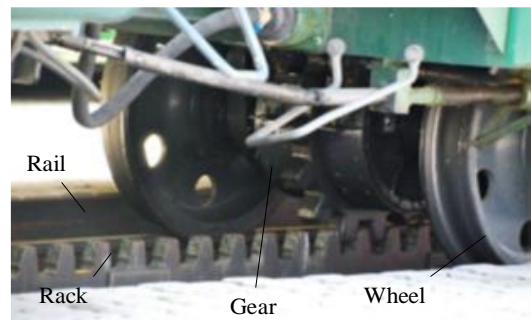


Fig. 2 Structure of Strub type rack vehicle [7]

$$[M]\{\ddot{X}\} + [C]\{\dot{X}\} + [K]\{X\} = \{P\}, \quad (1)$$

where $[M]$, $[C]$ and $[K]$ are the generalized mass matrix, generalized damping matrix and generalized stiffness matrix of the whole rack vehicle system; $\{\ddot{X}\}$, $\{\dot{X}\}$ and $\{X\}$ are the generalized acceleration matrix, velocity matrix and displacement matrix of the rack vehicle; $\{P\}$ is the generalized

load vector. The detailed derivation process and equation of motion can refer to the author's previous research literature [5, 23, 24].

The wheel/rail nonlinear contact is simulated by Hertz nonlinear elastic contact theory and Kalker linear creep theory with the consideration of relative displacement between wheel and rail [25].

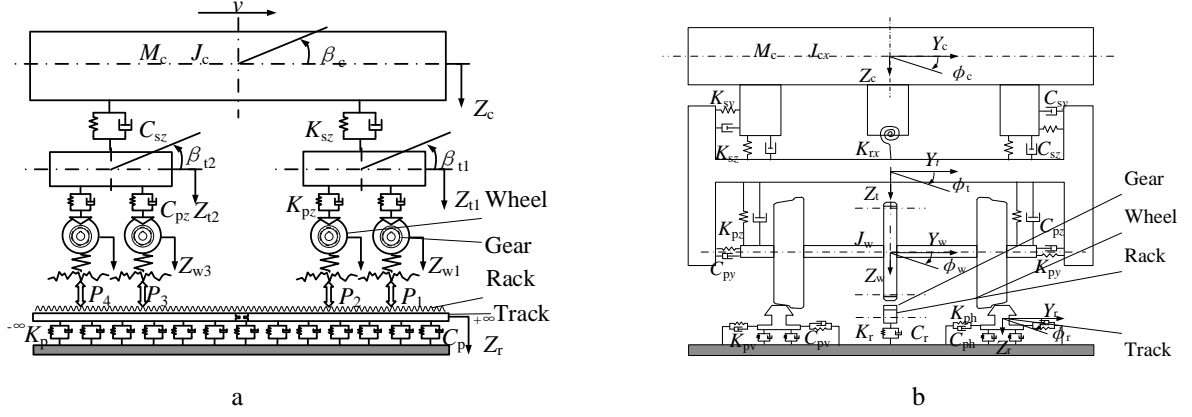


Fig. 3 Rack vehicle dynamic model: a – side view; b – end view

Table 1

DoF of vehicle model

DoF	Longitudinal	Lateral	Vertical	Rolling	Yawing	Rotation
Carbody	/	Y_c	Z_c	ϕ_c	ψ_c	β_c
Frame($i=1,2$)	/	Y_t	Z_t	ϕ_t	ψ_t	β_t
Wheelset($i=1,2,3,4$)	/	Y_w	Z_w	ϕ_w	ψ_w	β_w
Driving gear($i=1,2,3,4$)	X_g	/	Z_g	/	/	θ_g

2.3. Gear-rack meshing system model

Without considering the influence of time-varying factors such as gear backlash, a five degree of freedom dynamic meshing model of gear-rack is established, as shown in Fig. 4, in which the y -axis is along the direction of the meshing line. The moment of inertia, torque and torsional angle displacement of the driving gear in the figure are I_g , T_g , θ_g ; X_h and Z_h are the circumferential and radial displacement of the rack relative to the gear; K_{xg} , C_{xg} , K_{zg} and C_{zg} are the bearing stiffness and damping of the model in the longitudinal and vertical directions of the system

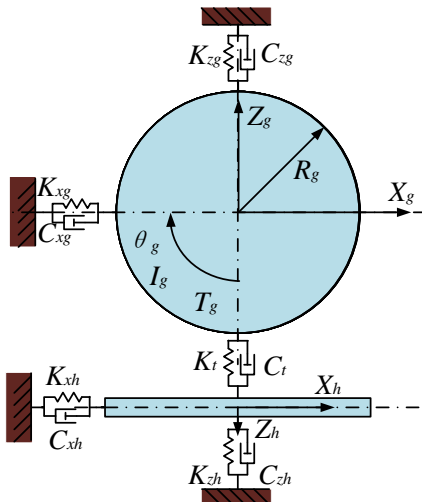


Fig. 4 Gear-rack meshing mode

respectively; K_{xh} , C_{xh} , K_{zh} and C_{zh} represent the stiffness and damping of fasteners fixed on the rack in the longitudinal and vertical directions.

Based on the five degree of freedom model of gear-rack and Newton's law of motion, the dynamic differential equation is established.

$$I_g \ddot{\theta}(t) = T_g - \sum_{i=1}^2 r_{bg} F_{dpi}(t), \quad (2)$$

$$M_g \ddot{Z}_g(t) + C_{zg} \dot{Z}_g(t) + K_{zg} Z_g(t) + \sum_{i=1}^2 F_{dpi} = 0, \quad (3)$$

$$M_h \ddot{Z}_h(t) + C_{zh} \dot{Z}_h(t) + K_{zh} Z_h(t) + \sum_{i=1}^2 F_{dpi} = 0, \quad (4)$$

$$M_g \ddot{X}_g(t) + C_{xg} \dot{X}_g(t) + K_{xg} X_g(t) + \sum_{i=1}^2 F_{fpi} = 0, \quad (5)$$

$$M_h \ddot{X}_h(t) + C_{xh} \dot{X}_h(t) + K_{xh} X_h(t) + \sum_{i=1}^2 F_{fpi} = 0, \quad (6)$$

where Z_g and X_g are the displacement of the gear in the longitudinal and vertical directions, Z_h and X_h are the displacement of the rack in the longitudinal and vertical directions, r_{bg} is the radius of the base circle of the gear, F_{dpi} and F_{fpi} are the dynamic contact force and dynamic friction force of the gear rack.

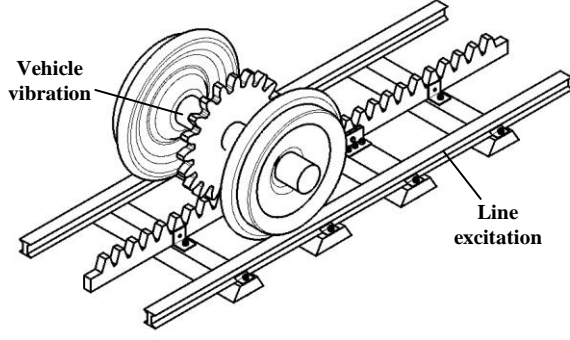


Fig. 5 Gear and axle connection

In addition, as shown in Fig. 5, the driving gear is connected with the axle. In the actual operation process,

$$F_t = (F_{dpi} - F_{dpi}^*) \times \left\{ 1 + \frac{K_1(t^*) K_2(t^*) \left[K_1 \left(t^* + \frac{\Delta\varphi}{\omega_1} - T_z \right) \cos \Delta\gamma + K_2(t^* + T_z) \right]}{K_1 \left(t^* + \frac{\Delta\varphi}{\omega_1} - K_2 \right) K_2(t^* + T_z) \left[K_1(t^*) + K_2(t^*) \right]} \right\}, \quad (8)$$

where F_{dpi} is the dynamic contact force of gear teeth; F_{dpi}^* is the force between the first pair of teeth before the latter pair of gears enter meshing; $K_1(t^*)$, $K_2(t^*)$ are the pitch stiffness of the meshing point between the driving gear and the rack at time t^* ; $\Delta\varphi$ is the change of meshing angle of driving gear caused by the change of meshing point; $\Delta\gamma$ is the sum of the changes in the meshing angle between the driving gear and the rack under corresponding conditions.

2.4. Carbody gravity center offset model

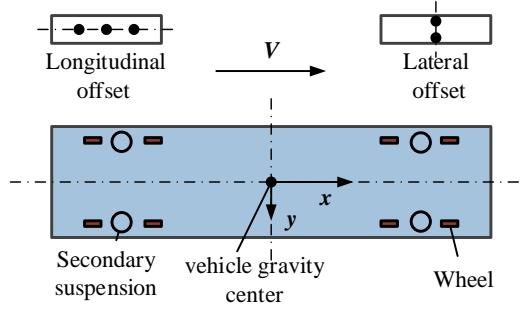


Fig. 6 Carbody gravity center offset model

The gravity center of the unbiased carbody at the geometric center of the vehicle body is set, and the carbody gravity center subjected to offset will be offset at the geometric center of the plane. The offset geometric coordinates of the center of gravity of the carbody is set to (x, y) , as shown in Fig. 6.

The carbody moment balance equation is listed

$$M_c g (l_c + x) = 2l_c F_{wF2}, \quad (9)$$

$$M_c g (l_h + y) = 2l_h F_{wR2}, \quad (10)$$

where M_c is the mass of the carbody, l_c is the half of the fixed distance of the carbody, l_h is the half of the rolling circle span, F_{wF2} is the sum of the vertical forces on the front bogie wheels of the carbody, and F_{wR2} is the sum of

due to the influence of the vibration of the rack vehicle or the line excitation, the rack and the driving gear are prone to meshing error, which further leads to meshing impact.

Considering the meshing error, the meshing time will change. Therefore, starting from the meshing impact time, the difference between the theoretical meshing time and the actual meshing time is defined as

$$\Delta t = T_z - t_0, \quad (7)$$

where T_z is the theoretical meshing time, $T_z = 2\pi/z_1\omega_1$, z_1 is the number of driving gear teeth, ω_1 is the rotational angular speed of the driving gear, and t_0 is the actual meshing time.

Normally, Δt is about (5~10) % of T_z , and the meshing impact force at time t can be obtained.

the vertical forces on the four wheels on the carbody right side.

According to Eqs. (9) (10), the initial force on the left and right wheels of the front and rear bogies during static balance is calculated

$$F_{wFR} = Mg \left(1 + \frac{x}{l_c} - \frac{y}{l_h} \right) / 8 + M_{t1} / 4, \quad (11)$$

$$F_{wFL} = Mg \left(1 + \frac{x}{l_c} + \frac{y}{l_h} \right) / 8 + M_{t1} / 4, \quad (12)$$

$$F_{wTR} = Mg \left(1 - \frac{x}{l_c} - \frac{y}{l_h} \right) / 8 + M_{t2} / 4, \quad (13)$$

$$F_{wTL} = Mg \left(1 - \frac{x}{l_c} + \frac{y}{l_h} \right) / 8 + M_{t2} / 4, \quad (14)$$

where F_{wFR} is the vertical force on the right wheel of the front bogie, F_{wFL} is the vertical force on the left wheel of the front bogie, F_{wTR} is the vertical force on the right wheel of the rear bogie, F_{wTL} is the rear bogie the vertical force on the left wheel, M_{t1} and M_{t2} are the masses of the front and rear bogies. The uneven force on the wheelset is more serious when the offset of the center of gravity is larger.

2.5. Model verification

In order to verify the accuracy of the rack vehicle model, this paper designed and implemented an experimental test on a rack-railway line in Chongqing Dazu. The gear-rack contact force and carbody vertical acceleration were tested, and some of the measured sites are shown in Fig. 7, a - c.

It can be seen from Fig. 7, a-c that the produced results of the model in this paper are close to the test results, which proves that the dynamic model of rack vehicle in this paper is correct.

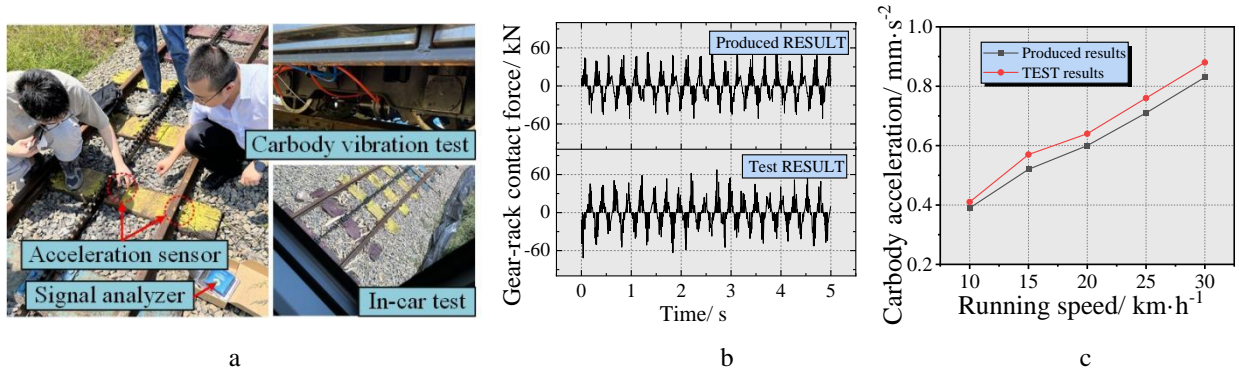


Fig. 7 Field measurement and result comparison: a – field measurement, b – gear-rack nonlinear contact force, c – carbody acceleration

3. Calculation Conditions and Parameters

In rack railway engineering, the application of gear-rack meshing driving section curve is not common, and in order to clearly reflect the impact of the carbody gravity center offset on the dynamic characteristics of the system, the follow-up research does not consider the influence of the curve line and random irregularities in the track.

The working condition are set as shown in Table 2. In this paper, the rack vehicle system dynamic behavior is studied by changing the lateral and longitudinal offsets of the carbody gravity center.

Working condition

Subject	Numerical value	Unit
Slope	10%	/
Speed	30	km/h
lateral offset	-0.3~0.3	m
longitudinal offset	-3~3	m

Table 2

Research indicators

Dynamic characteristics	Parameter index	Limitation
Gear meshing characteristics	Dynamic contact force f_{dpi}	/
	Gear dynamic performance	/
	Gear radial meshing offset	20 mm
Vehicle safety	Wheel rail vertical force P	/
	Axle lateral force H	$15+P/3$ kN
	Wheel unloading rate $\Delta P/P$	0.65
	Derailment factor	0.8
Vehicle stability	Body acceleration a_c	2.5 m/s ²
	Vertical Sperling W	3.0

Table 3

In order to adapt to the mountain route conditions, the structure of the rack vehicle is generally smaller than that of the traditional rail vehicle. The main structural parameters of the rack vehicle are shown in Table 4.

The driving gear and bogie axle connected by bearings, and the meshing of the gear-rack directly affects the wheel/rail action. Therefore, it is necessary to study the

meshing characteristics of the gear-rack before studying the rack vehicle dynamic characteristics. In addition, the carbody gravity center offset mainly affects the safety and stability of the rack vehicle. This paper mainly explores the effect of the carbody gravity center offset on the wheel/rail vertical force, axle lateral force, wheel unloading rate, derailment factor, body acceleration and Sperling index. The selection of research indicators for the dynamic behavior of rack vehicles is shown in Table 3.

Rack vehicle parameters

Table 4

Subject	Number	Unit
Maximum speed	30	km/h
Carbody size	16×3.2×3.4	m
Carbody weight	3.2×10^4	kg
Carbody pitching inertia	2×10^6	kg·m ²
Vehicle distance	11.6	m
Bogie width	1.8	m
Frame weight	580	kg
Bogie wheelbase	2.8	m
Gear module	32	mm
Teeth	22	/
Gear width	60	mm
Rack width	80	mm
Pressure angle	20	°
Rolling circle span	1058	mm
Nominal rolling radius	0.42	m
Secondary suspension span	1.72	m

4. Gear-Rack Nonlinear Meshing Behavior Subject to Carbody Gravity Center Offset

The influence of different gravity center offsets on the nonlinear meshing behavior of gear-rack is mainly explored in this chapter.

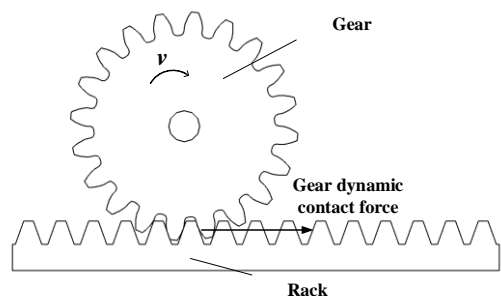


Fig. 8 Schematic diagram of gear-rack

As shown in Fig. 8, the gear-rack dynamic contact force is the force that the gear rack meshes to provide traction for the vehicle during the driving process.

4.1. Gear-rack dynamic contact force

The gear-rack dynamic contact force affected by the no gravity center offset (NO), the lateral offset (LA) by

0.2 m and the longitudinal offset (LO) by 3.0 m when the rack vehicle runs at the speed of 10 and 30 km/h on the slope are respectively presented in Fig. 9, a-b and Fig. 10, a-b is the numerical distribution diagram of the gear-rack dynamic contact force when the rack vehicle runs at the speed of 10 and 30 km/h on the slope.

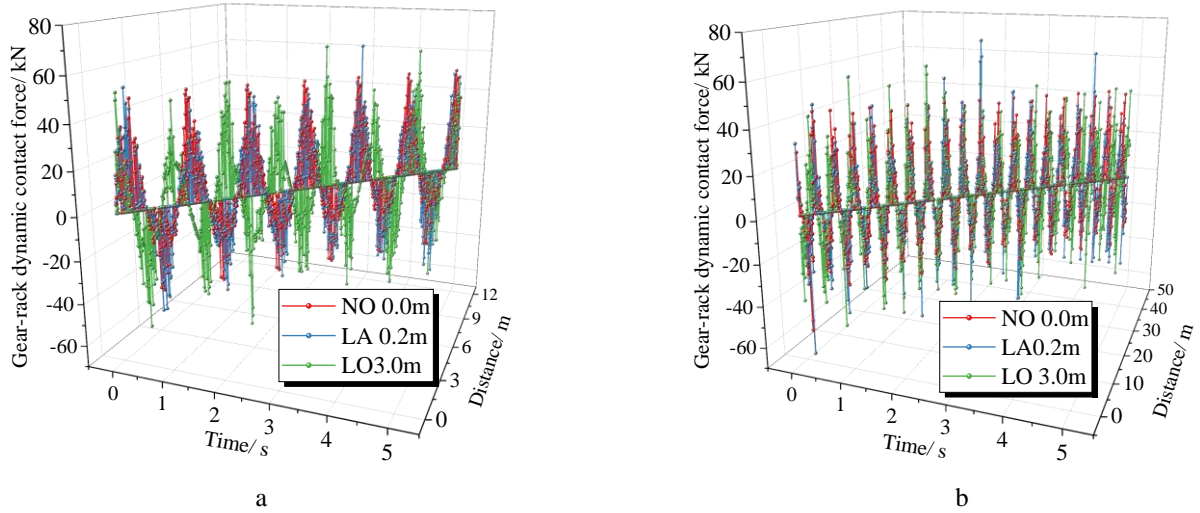


Fig. 9 Gear-rack dynamic contact force: a – contact force at 10 km/h, b – contact force at 30 km/h

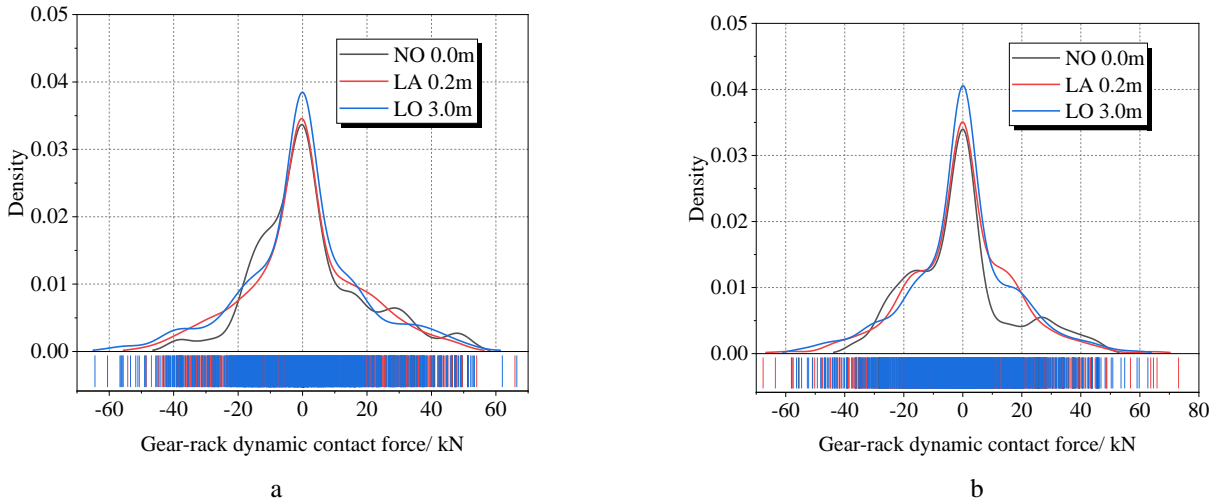


Fig. 10 Numerical distribution diagram of contact force: a – contact force at 10 km/h, b – contact force at 30 km/h

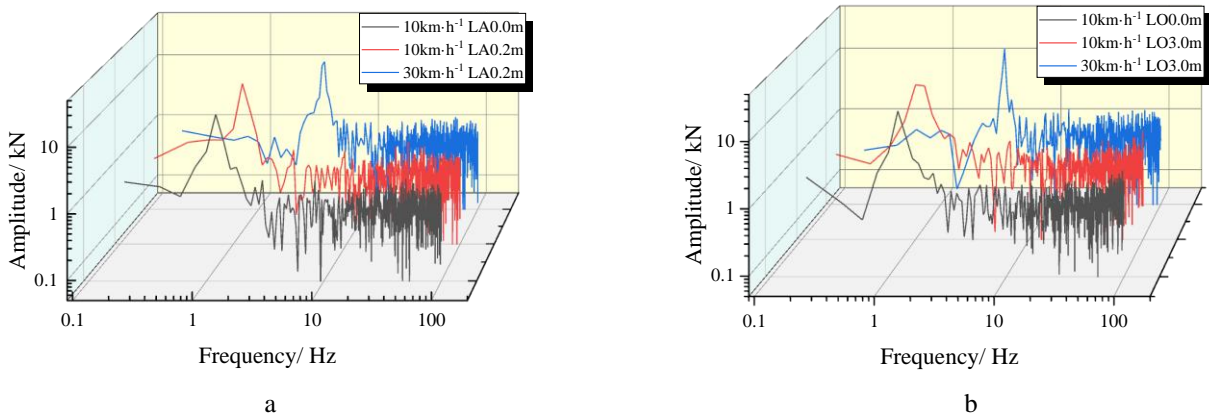


Fig. 11 Gear-rack dynamic contact force (PSD): a – contact force under lateral offset, b – contact force under longitudinal offset

The lateral and longitudinal offset of the rack vehicle carbody gravity center have a certain impact on the gear-rack dynamic contact force can be seen from Fig. 9, a-b and Fig. 10, a-b. The appearance of offset makes the gear-rack dynamic contact force produce great impact, and the impact becomes more obvious with the increase of speed. The amplitude of gear-rack dynamic contact force remains about 43 kN when there is no gravity center offset, which is impacted by the coupling interference of multiple gears. The gear-rack dynamic contact force reaches the maximum value of 73 kN when the speed reaches 30 km/h.

Fig. 11, a is the frequency domain curve of the gear-rack dynamic contact force affected by the rack vehicle carbody gravity center lateral offset. Fig. 11, b is the frequency domain curve of the dynamic contact force of the

gear affected by the rack vehicle carbody gravity center longitudinal offset.

As shown in Fig. 11, a-b, the gear-rack dynamic contact force is not significantly affected by carbody gravity center offset, but significantly affected by the rack vehicle running speed. When the speed is 10 km/h, the frequency is 0.9, and the frequency is 3.9 when the speed is 30 km/h.

4.2. Gear-rack nonlinear dynamic characteristic

The longitudinal acceleration of rack vehicle driving gear is shown in Fig. 12, a. With the consideration that there is no characteristic peak after 100 Hz, the frequency band of 1~100 Hz is taken out for research.

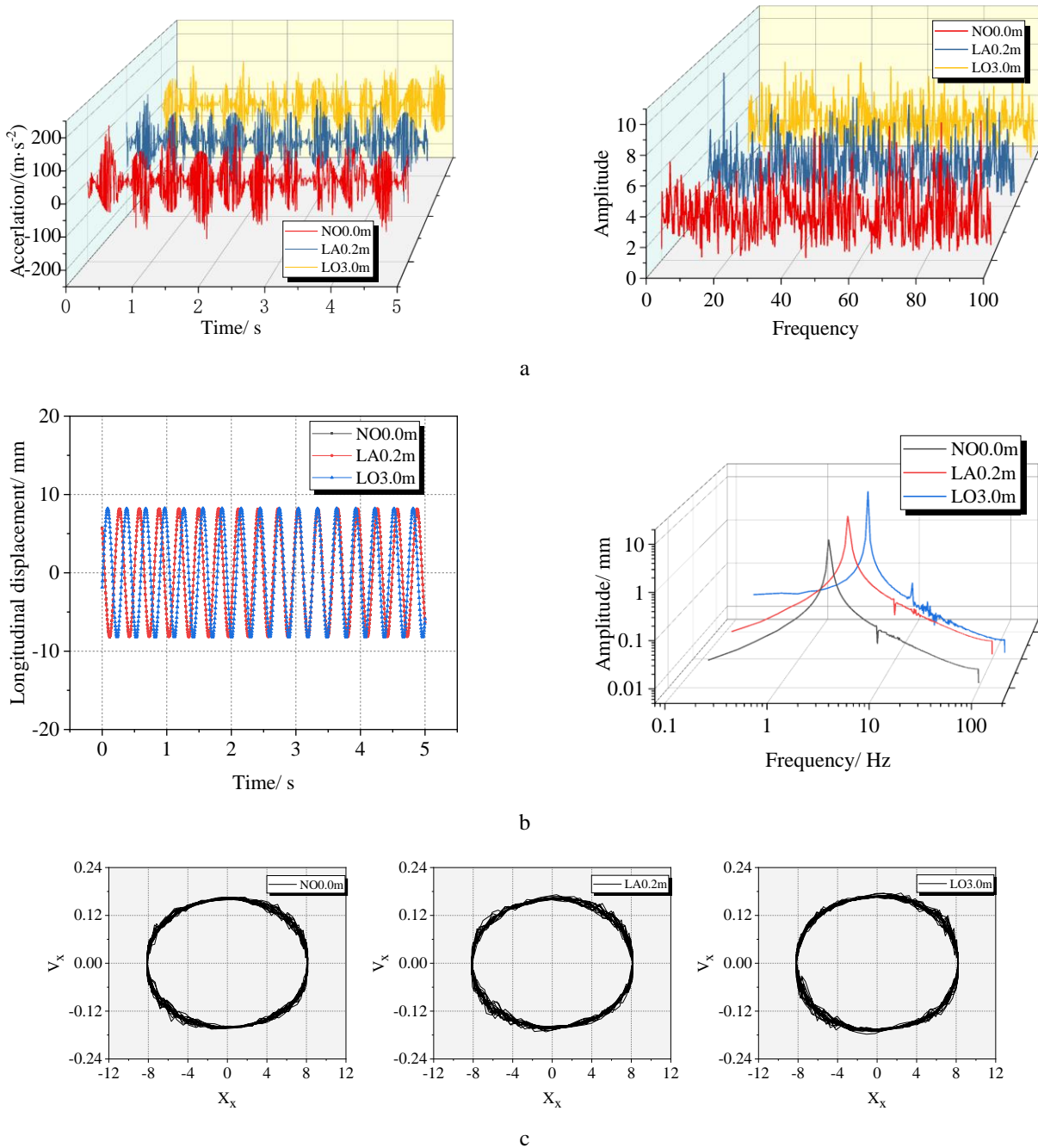


Fig. 12 Gear-rack nonlinear dynamic characteristics: a – gear longitudinal acceleration in time-domain and frequency-domain, b – gear time history in time-domain and frequency-domain, c – gear phase diagram

It can be seen that the gear acceleration curves subject to the three gravity center offset modes are very similar, which means that the longitudinal vibration of the driving gear is less affected by the carbody gravity offset. The results of frequency analysis show that the peak value of gear vibration occurs at 16.7 Hz, 39.4 Hz, and 85.2 Hz.

Since the unbalance load caused by the carbody gravity center offset is mainly borne by the wheelset installed on both sides of the axle, the gravity center offset has little effect on the gear time history. As shown in Fig. 12, b, the gear time history is almost the same, and the main influence frequency is 3.8 Hz. The nonlinear gear system in periodic motion can be seen from in Fig. 12, c, and the gear phase diagram is a non-circular closed curve with a certain width. According to the time response diagram, the gear-rack system is in a unilateral impact state.

4.3. Gear radial mesh offset

The gear radial mesh offset is the radial error between the gear and rack caused by the wheelset lateral movement, Fig. 13 shows the gear radial mesh offset curve when the carbody is no gravity center offset, lateral offset 0.3 m and longitudinal offset 3.0 m. It can be clearly observed that the carbody gravity center longitudinal offset has little effect on the gear radial mesh offset, the lateral offset has a greater effect. When the lateral offset is 0.3 m, the gear radial mesh offset reaches 0.11 mm.

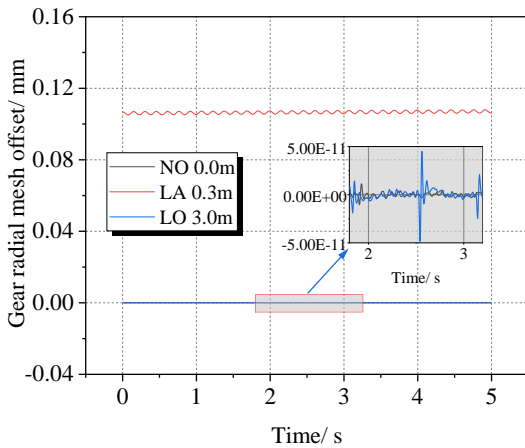


Fig. 13 Gear radial mesh offset

5. Vehicle Safety Characteristics Subject to Carbody Gravity Center Offset

The influence of the carbody gravity center lateral offset and longitudinal offset on the vehicle safety characteristics when the rack vehicle is running on the slope at speeds of 10, 20, and 30 km/h is investigated.

5.1. Wheel/rail vertical force

The maximum vertical force of the left and right wheel affected by the lateral offset of the carbody gravity center is shown in Fig. 14, and Fig. 15 shows the wheel/rail vertical force on the load-increasing side when the rack vehicle with no offset and 0.2 m lateral offset runs at 10, 20, and 30 km/h.

In Fig. 14 the maximum vertical force is greatly affected by the lateral offset of the carbody gravity center.

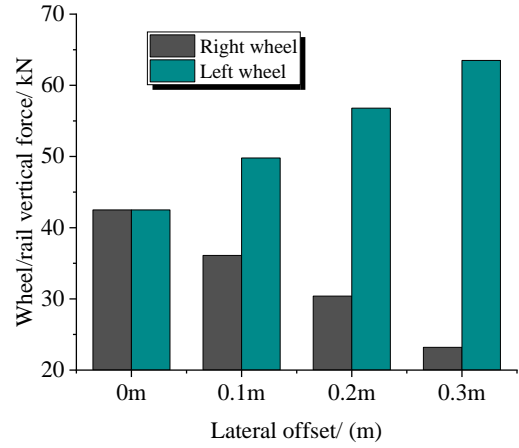


Fig. 14 Maximum wheel/rail vertical force

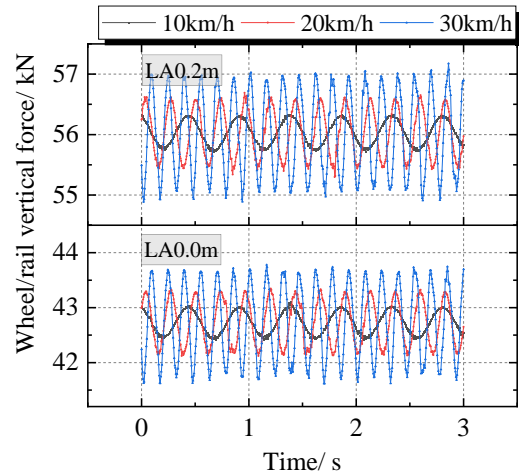


Fig. 15 Wheel/rail vertical force in time-domain

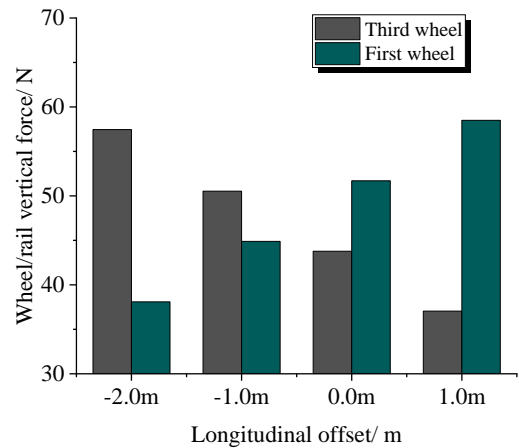


Fig. 16 Maximum wheel/rail vertical force

With the increase of the lateral offset, the eccentric load phenomenon of the left and right wheels becomes more obvious, the load-increasing side reaches 63.5 kN. It can be seen from Fig. 15 that the lateral offset of the center of gravity of the vehicle has little effect on the amplitude and frequency of the wheel/rail vertical force, and is significantly affected by the running speed of the vehicle, and the faster the speed, the greater the vibration frequency and amplitude. This phenomenon is caused by gear-rack meshing impact.

Fig. 16 shows the maximum wheel/rail vertical force of the first wheelset and the third wheelset with a

carbody gravity center longitudinal offset from -2 m to 1 m when the rack vehicle runs at a speed of 30 km/h. Fig. 17 shows the wheel/rail vertical force of the third wheelset with a forward 1 m deviation and a rear 2.0 m deviation when the rack vehicle running at 10, 20, and 30 km/h.

In Fig. 16 and Fig. 17, can see that the rack vehicle carbody gravity center longitudinal offset has a linear effect on the wheel/rail vertical force of the front and rear wheels. When the carbody gravity center is offset backwards, the wheel/rail vertical force of the third wheel increases, and the first wheel wheel/rail vertical force decreases. The wheel/rail vertical force vibration frequency and amplitude are affected by the running speed, and the frequency and amplitude increase with the speed.

5.2. Axle lateral force

Fig. 18, a-b shows the axle lateral force subject to the rack vehicle runs at the speed of 10, 20 and 30 km/h under the condition that the carbody gravity center laterally offset by 0.2 m.

It can be directly seen from Fig. 18, a-b that when the rack vehicle carbody gravity center is offset laterally by 0.2 m, the average value of the axle lateral force is

923 N. The amplitude and frequency of axle lateral force are affected by the carbody gravity center lateral offset and running speed. In addition, the faster the running speed, the greater the axle lateral force floating, and the faster the axle lateral force frequency. When the speed is 30 km/h, the main influence frequency is 6.6Hz.

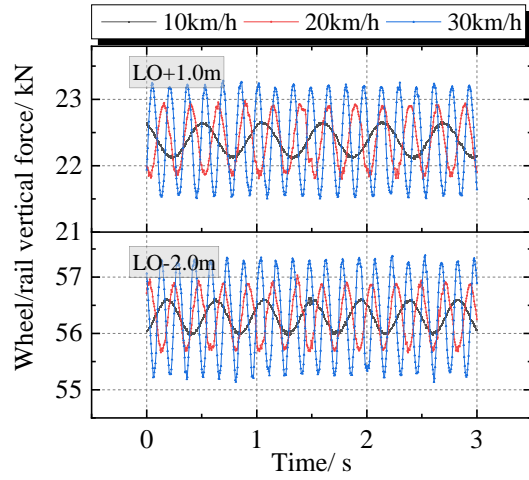
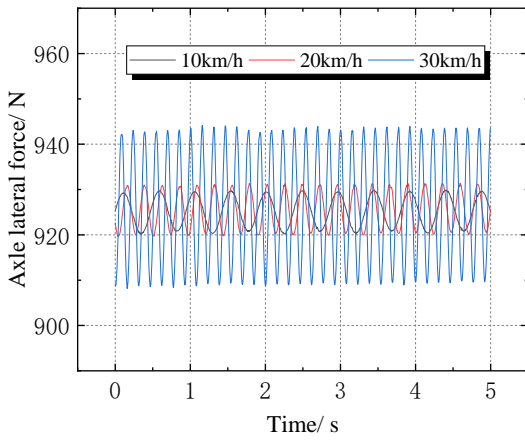
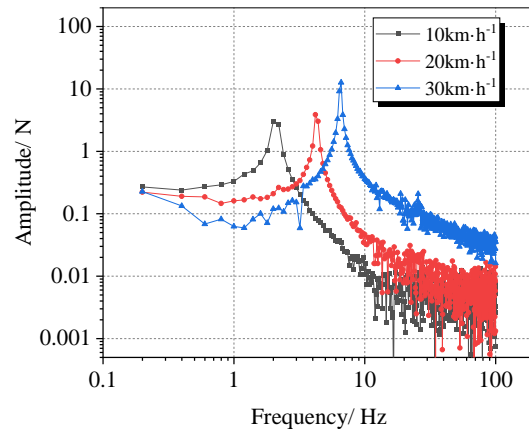


Fig. 17 Wheel/rail vertical force in time-domain

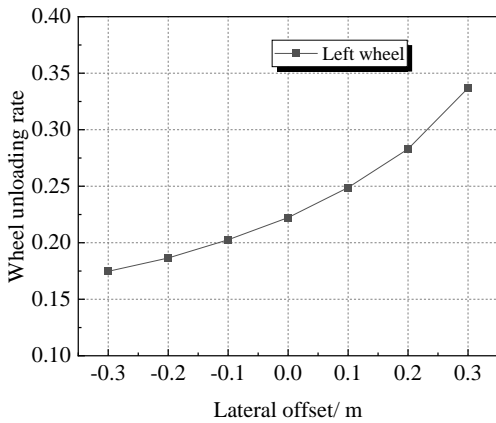


a

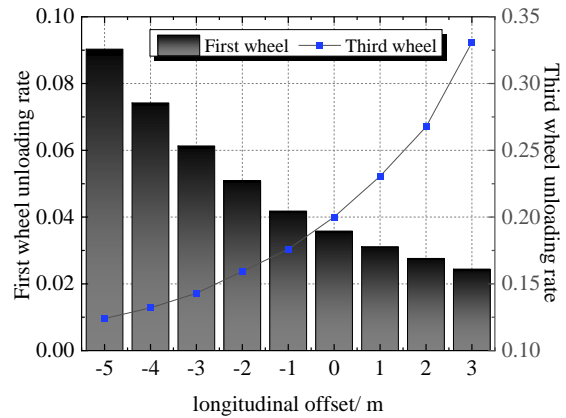


b

Fig. 18 Axle lateral force: a – time domain, b – frequency domain



a



b

Fig. 19 Wheel unloading rate subject to offset: a – wheel unloading rate under lateral offset, b – wheel unloading rate under longitudinal offset

5.3. Wheel unloading rate

Fig. 19, a show the effect of the lateral offset on the wheel unloading rate of the rack vehicle, and Fig. 19, b shows the effect subject to the longitudinal offset.

As shown in Fig. 19, a that the influence of the carbody gravity center lateral offset on the wheel unloading rate is symmetrically distributed, when the lateral right deviation is 0.3m, the wheel unloading rate reaches 0.34. It can be seen from Fig. 19, b that the wheel unloading rate on the load-reducing side increases with the carbody gravity center longitudinal offset. The third wheel's wheel unloading rate reaches 0.33 when the longitudinal forward deviation is 3m. and compared with the first wheelset, the wheel load reduction phenomenon of the third wheelset is more significant, which is caused by the greater influence of the bogie load at the rear end of the slope. When the gravity center is 3 m behind, the rack vehicle wheel unloading rate reaches the best.

5.4. Derailment coefficient

Fig. 20, a-b respectively show the influence of the carbody gravity center lateral and longitudinal offset on the rack vehicle's derailment coefficient.

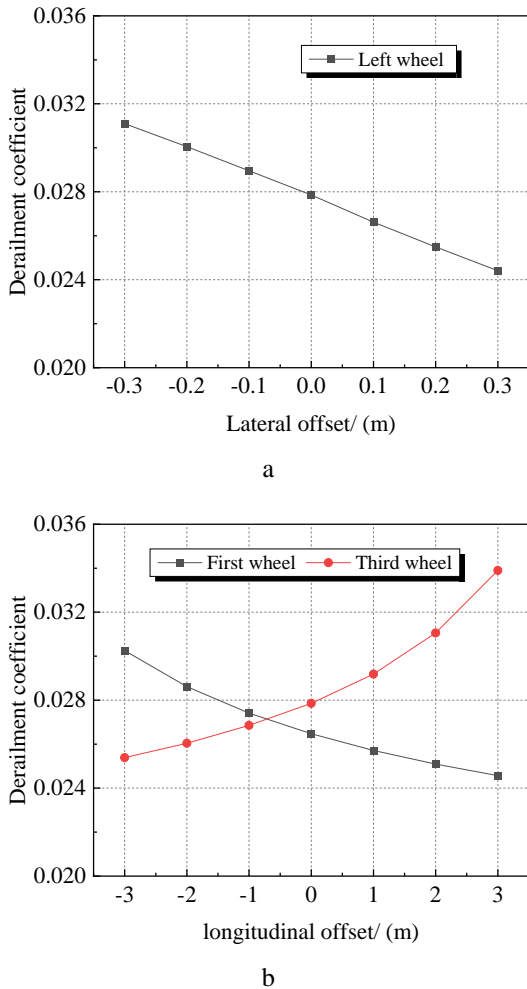


Fig. 20 Derailment coefficient subject to offset: a – derailment coefficient under lateral offset, b – derailment coefficient under longitudinal offset

As we can see in Fig. 20, a-b that the variation trend of the derailment coefficient under the lateral and longitudinal offset is similar to the wheel unloading rate.

The influence of the lateral offset on the derailment coefficient on the increased or decreased load side is distributed linearly and symmetrically. The increase of longitudinal offset increases the derailment coefficient of the wheelset on the load shedding side, and the derailment coefficient of the wheelset on the load shedding side is more sensitive to the offset.

6. Vehicle Stability Characteristics Subject to Carbody Gravity Center Offset

The influence of the carbody gravity center lateral and longitudinal offset on the vehicle stability characteristics when the rack vehicle is running on the slope at speeds of 10, 20, and 30 km/h is investigated.

6.1. Carbody vertical acceleration

Fig. 21 shows the carbody vertical acceleration of the rack vehicle affected by the lateral offset at a running speed of 30 km/h. Fig. 22 is a graph showing the influence of the carbody gravity center lateral offset on the rack vehicle carbody vertical acceleration.

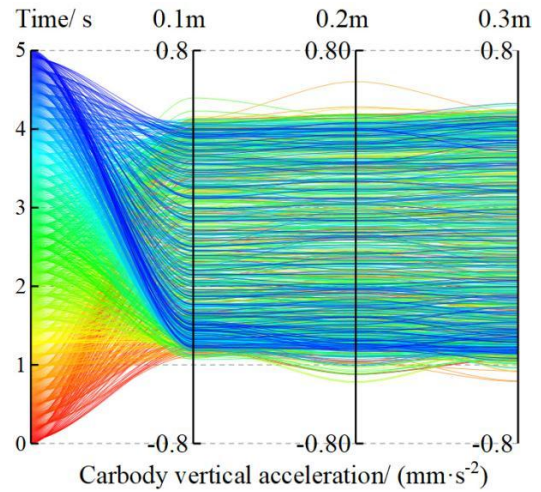


Fig. 21 Carbody vertical acceleration in time domain

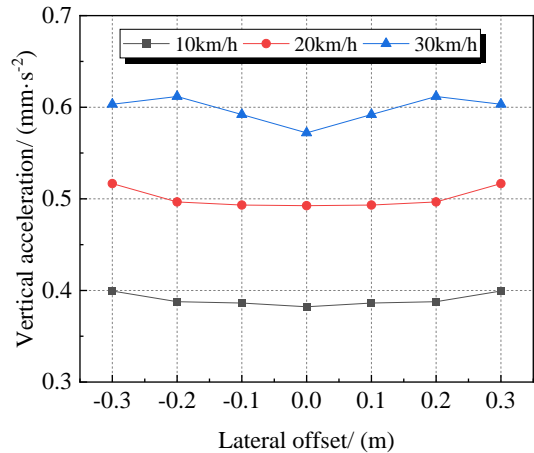


Fig. 22 Carbody vertical acceleration

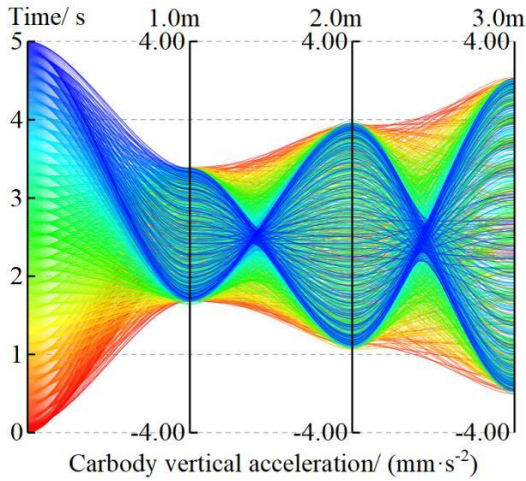


Fig. 23 Carbody vertical acceleration in time domain

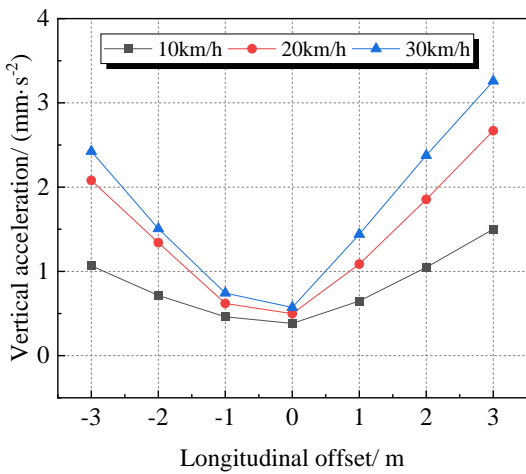


Fig. 24 Carbody vertical acceleration

As shown in Fig. 21 and Fig. 22, the carbody gravity center lateral offset has a certain influence on the carbody vertical acceleration, and the vehicle running speed has a significant impact on the carbody vertical acceleration. The carbody vertical acceleration decreases with the decrease of lateral offset and running speed.

Fig. 23 shows the rack vehicle carbody vertical acceleration affected by the carbody gravity center longitudinal offset at a running speed of 30 km/h. Fig. 24 is a graph showing the influence of the carbody gravity center longitudinal offset on the carbody vertical acceleration.

As shown in Fig. 23, the carbody vertical acceleration is extremely sensitive to the carbody gravity center longitudinal offset. It can be seen from Fig. 24 that the vertical acceleration reaches the minimum value at the gravity center longitudinal position from -1 to 0 m, the vehicle running speed has a significant influence on the carbody vertical acceleration, and the vertical acceleration increases with the increase of speed.

6.2. Vehicle vertical Sperling index

Fig. 25, a-c respectively shows the influence of the rack vehicle carbody gravity center lateral and longitudinal offset on the vertical Sperling index under the running speed of the rack vehicle is 10, 20, and 30 km/h.

As it can be seen in Fig. 25, a-c, the vertical Sperling index is significantly affected by the gravity center longitudinal offset of the rack vehicle, and the minimum value is reached at 0-1m longitudinally behind the gravity center the rack vehicle; In addition, the running speed of the rack vehicle has a certain influence on the vertical Sperling index. As the running speed of the vehicle increases, the Sperling index gradually increases, and is more sensitive to the influence of the lateral offset of the gravity center.

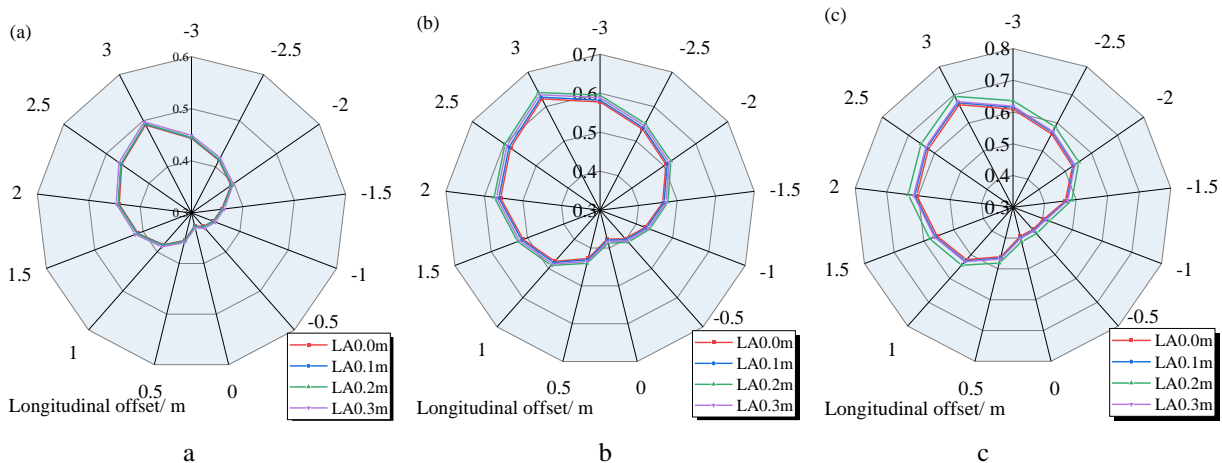


Fig. 25 Vertical Sperling index at difference speed: a – Sperling at 10 km/h; b – Sperling at 20 km/h; c – Sperling at 30 km/h

7. Conclusions

In this study, aiming at the influence of gear-rack meshing impact disturbance on wheel/rail action behavior, the mechanism of meshing disturbance was explored through Gear dynamics. On this basis, the coupling model of the rack vehicle system is established. Selected three working conditions of high, medium and low running speed on the slope to study the gear-rack nonlinear mesh-

ing behavior and the dynamic characteristics of rack vehicle subject to the carbody gravity center offset, and analyze its safety and stability. The main conclusions from the above studies are as follows:

1. The method is effective for studying the rack vehicle dynamic characteristics subject to the carbody gravity center offset. Under the offset, the gear-rack nonlinear meshing impact disturbance has a significant impact on the operation of the vehicle. The gear-rack dynamic

contact force is affected by the running speed of rack vehicle and carbody gravity center offset.

2. For the parameters selected in this paper, the wheel/rail vertical force is influenced by the carbody gravity center offset, and is affected by the gear-rack meshing significantly. The axle lateral force and the wheel unloading rate is increase with the change of lateral offset of the carbody gravity center.

3. For the parameters selected in this paper, the carbody vertical acceleration and the vertical Sperling index are greatly affected by the longitudinal offset of the carbody gravity center. The faster the running speed, the more serious the longitudinal offset affects the vertical Sperling index. The vertical Sperling index is optimal when the carbody gravity center is placed 0~1m behind.

4. The safety and stability of rack vehicle are not only affected by the gear-rack nonlinear meshing, but also the safety is affected by the carbody gravity center lateral offset, and the stability is affected by the carbody gravity center longitudinal offset.

Declaration of Conflicting Interests

The author declares no conflict of interest in preparing this article.

Acknowledgement

This work was supported by the National Natural Science Foundation of China [Grant Number: 52008067], the Sichuan Science and Technology Program [2021YFG0211].

References

- Hansen, B.** 2009. Gearing Up: The Mount Washington Cog Railway, *Civil Engineering Magazine Archive* 79(4): 36-39.
<https://doi.org/10.1061/ciegag.0000525>.
- Yu, H.; Zhang, Y.; Chen, L.** 2020. Research on technical characteristics and application prospect of track railway, *Journal of Railway Engineering Society (in Chinese)* 37(10): 6-10.
- Loomis, J.; Keske, C.** 2009. The Economic Value of Novel Means of Ascending High Mountain Peaks: A Travel Cost Demand Model of Pikes Peak Cog Railway Riders, Automobile Users and Hikers, *Tourism Economics* 15(2): 426-436.
<https://doi.org/10.5367/000000009788254313>.
- Liu, Y.; Hong, T.; Li, Z.** 2020. Influence of Toothed Rail Parameters on Impact Vibration Meshing of Mountainous Self-Propelled Electric Monorail Transporter, *Sensors* 20(20): 5880.
<https://doi.org/10.3390/s20205880>.
- Chen, Z. W.; Li, S. H.** 2021. Dynamic evaluation and optimization of layout mode of traction motor in rack vehicle, *Nonlinear Dynamics* 106: 3025-3050.
<https://doi.org/10.1007/s11071-021-06939-6>.
- Guo, F.; Wu, S. C.; Liu, J. X.; Zhang, W.; Qin, Q. B.; Yao, Y.** 2020. Fatigue life assessment of bogie frames in high-speed railway vehicles considering gear meshing, *International Journal of Fatigue* 132: 105353.
<https://doi.org/10.1016/j.ijfatigue.2019.105353>.
- Chen, S. X.; Lin, J. H.** 2014. Nonlinearity and non-stationarity analysis of dynamic response of vehicle-track coupling system enhanced by Huang transform, *Measurement* 55: 305-317.
<https://doi.org/10.1016/j.measurement.2014.05.023>.
- Han, J.; Zhao, G. T.; Xiao, X. B.; Wen, Z. F.; Guan, Q. H.; Jin, X. S.** 2015. Effect of softening of cement asphalt mortar on vehicle operation safety and track dynamics, *Journal of Zhejiang University - Science A* 16: 976-986.
<https://doi.org/10.1631/jzus.A1500080>.
- Wang, W.; Liang, Y.; Zhang, W.; Iwnicki, S.** 2019. Effect of the nonlinear displacement-dependent characteristics of a hydraulic damper on high-speed rail pantograph dynamics, *Nonlinear Dynamics* 95: 3439-3464.
<https://doi.org/10.1007/s11071-019-04766-4>.
- Zhang, L.** 2017. Vehicle-track vertical coupling dynamics on dip-joint and corrugation rails, Hong Kong Polytechnic University. Master thesis. 56p. Available at:
<https://theses.lib.polyu.edu.hk/handle/200/9019>.
- Yu, W.; Shao, Y.; Mechefske, C. K.** 2015. The effects of spur gear tooth spatial crack propagation on gear mesh stiffness, *Engineering Failure Analysis* 54: 103-119.
<https://doi.org/10.1016/j.engfailanal.2015.04.013>.
- Wei, S.; Han, Q. K.; Dong, J.; Peng, Z. K.; Chu, F. L.** 2017. Dynamic response of a single-mesh gear system with periodic mesh stiffness and backlash nonlinearity under uncertainty, *Nonlinear Dynamics* 89: 49-60.
<https://doi.org/10.1007/s11071-017-3435-z>.
- Cooley, C. G.; Liu, C.; Dai, X.; Parker, R. G.** 2016. Gear tooth mesh stiffness: A comparison of calculation approaches, *Mechanism and Machine Theory* 105: 540-553.
<https://doi.org/10.1016/j.mechmachtheory.2016.07.021>.
- Pei, J.; Han, X.; Tao, Y.; Feng, S.** 2021. Lubrication reliability analysis of spur gear systems based on random dynamics, *Tribology International*, 153:106606.
<https://doi.org/10.1016/j.triboint.2020.106606>.
- Chen, J.; Li, W.; Sheng, L.; Jiang, S.; Li, M.** 2020. Study on reliability of shearer permanent magnet semi-direct drive gear transmission system, *International Journal of Fatigue*, 132(Mar.):105387.1-105387.12.
<https://doi.org/10.1016/j.ijfatigue.2019.105387>.
- He, G. Q.; Deng, S. J.; He, Y.; Yan, H. Z.; Sun, N.; Wang, Q. L.** 2016. Simulation Analysis of the Influence of Tooth Surface Pit Morphology on the Dynamics Performance of Face Gear Mesh (in Chinese), *Journal of Mechanical Transmission* 40(04): 110-116.
- Neusser, Z.; Sopouch, M.; Schaffner, T.; Priebisch, H.** 2010. Multi-body Dynamics Based Gear Mesh Models for Prediction of Gear Dynamics and Transmission Error, *SAE Technical Paper* 2010-01-0897.
<https://doi.org/10.4271/2010-01-0897>.
- Bao, T.; Han, M.; Chen, C.; Chen, S. Y.** 2015. Study on the Relationship between Lateral Offset of the Center of Gravity of Goods C70 Gondola and the Derailment Coefficient, *Proceedings of the 2015 International Conference on Mechatronics, Electronic, Industrial and Control Engineering*: 1429-1433.
<https://doi.org/10.2991/meic-15.2015.328>.
- Wan, X.; Han, M.; Fang, Z.; Yang, N.** 2015. Study on

Lateral Vibration Offsets of freight cars Under the Condition of Shift of Center of freight Gravity on the Curve Track, Proceedings of the 2015 International Conference on Mechatronics, Electronic, Industrial and Control Engineering. Atlantis Press 361: 2352-5401. <https://doi.org/10.2991/meic-15.2015.83>.

19. **Zhang, D.; Tang, Y.; Peng, Q.; Dong, C.; Ye, Y.** 2021. Effect of mass distribution on curving performance for a loaded wagon, *Nonlinear Dynamics* 104: 2259-2273. <https://doi.org/10.1007/s11071-021-06386-3>.
20. **Li, X.** 2012. The Permit Lateral Offset of Wagon Gravity Center Based on Anti-Overturning Stability. *ICTE* 2011: 2749-2754. [https://doi.org/10.1061/41184\(419\)454](https://doi.org/10.1061/41184(419)454).
21. **Zhai, W. M.; Wang, K. Y.; Cai, C. B.** 2009. Fundamentals of vehicle-track coupled dynamics, *Vehicle System Dynamics*: 47(11): 1349-1376. <https://doi.org/10.1080/00423110802621561>.
22. **Chen, Z. W.** 2021. Dynamic contact between CRTS II slab track and bridge due to time-dependent effect of bridge and its influence on train-track-bridge interaction, *Engineering Structures* 234: 111974. <https://doi.org/10.1016/j.engstruct.2021.111974>.
23. **Chen, Z. W.; Fang, H.** 2019. An Alternative Solution of Train-Track Dynamic Interaction, *Shock and Vibration* 2019: 1859261. <https://doi.org/10.1155/2019/1859261>.

M. Yuan, Z. Chen, S. Li, Z. Chen, J. Yang

DYNAMIC BEHAVIOR OF RACK VEHICLE SYSTEM SUBJECT TO GRAVITY CENTER OFFSET

S u m m a r y

Dynamic behavior of rack vehicle system subject to gravity center offset is investigated in this work. Considering the disturbance effect of gear-rack meshing impact and wheel/rail dynamic contact behavior, a complete dynamic model of rack vehicle is established based on multi-body dynamics, adopting which the influence of the carbody gravity center offset on the dynamic characteristics of rack vehicle and nonlinear meshing behavior of driven gear-rack system are explored. Results show that: The gear-rack dynamic contact force results in an impact under the rack vehicle carbody gravity center offset, and the impact increases with the increase of running speed. The gear-rack dynamic contact force reaches 73 kN when the speed reaches 30km/h. The lateral offset of the gravity center has a linear effect on rack vehicle running safety, and the wheel/rail vertical force is affected by the gear-rack dynamic meshing and produce vibration. The rack vehicle running stability is more sensitive to the longitudinal offset of the gravity center. The carbody acceleration increases by 4.8 times when the carbody gravity center is 3.0 m forward. The vertical Sperling index of the vehicle is optimal when the carbody gravity center is behind in 0~1 m. The conclusions of this study provide theoretical support for the worldwide rack railway design and safe operation.

Keywords: rack vehicle, gravity center offset, vehicle coupling dynamics, gear-rack meshing, nonlinear dynamics, safety and stability.

Received December 30, 2024

Accepted April 22, 2025



This article is an Open Access article distributed under the terms and conditions of the Creative Commons Attribution 4.0 (CC BY 4.0) License (<http://creativecommons.org/licenses/by/4.0/>).